https://doi.org/10.17221/27/2025-JFS

Assessing the accuracy of a root detector in mapping radial tree root distribution

*Mochammad Taufiqurrachman[1], Utami Dyah Syafitri[2], Goh Mia Chun[3], Lina Karlinasari[1]**

[1]Department of Forest Products, Faculty of Forestry and Environment, IPB University, Bogor, Indonesia
[2]Department of Statistics, Faculty of Mathematics and Natural Sciences, IPB University, Bogor, Indonesia
[3]CSK Landscape Services, Singapore

**Corresponding author: karlinasari@apps.ipb.ac.id*

Citation: Taufiqurrachman M., Syafitri U.D., Chun G.M., Karlinasari L. (2025): Assessing the accuracy of a root detector in mapping radial tree root distribution. J. For. Sci., 71: 406–415.

Abstract: A root detector is a non-destructive technology developed to indicate the radial distribution of tree roots, which are not often visible on the surface. This study aims to assess the accuracy of the root detector in estimating the radial distribution of both exposed and buried tree roots. Six *Agathis loranthifolia* Salisb. trees were selected, three with exposed roots and three with buried roots. The Fakopp® root detector, an acoustic-based tool, was used in this study. Root estimation was based on a combination of threshold values (> 400 $m \cdot s^{-1}$), average values, and the peak of the sound wave velocity. Soil excavation was manually conducted at a depth of 30 cm within a 100 cm radius of the tree trunk. The results showed that under similar soil conditions, the root detector achieved an accuracy of over 80% in detecting the actual radial root distribution, as validated by the excavation method. Root diameter exhibited the strongest correlation with sound velocity in detecting lateral roots. However, root depth and inclination angle contributed to detection inaccuracies in estimating the radial distribution of lateral roots.

Keywords: excavation method; lateral root; non-destructive method; sound velocity; validating

Trees play a crucial role in solving environmental problems, offering better air purification, heat reduction, shade, biodiversity, and thermal comfort than other vegetation types (Currie, Bass 2008; Abuseif, Gou 2018; Mughal, Corrao 2018; Muhammad et al. 2020; Abuseif et al. 2021). The root system, an often-overlooked component of a tree, plays a vital role in tree metabolism and stability (Buza, Divós 2016). In Smiley (2008), approximately 35% of tree failures are attributed to root-related issues according to the International Tree Failure Database (ITFD). Root distribution is critical for nutrient and water absorption as well as for mechanical anchorage, determining the tree's stability (Proto et al. 2020). Uneven root distribution (i.e. large sections without roots) can compromise a tree's ability to withstand wind forces and external loads (Watson et al. 2014).

Supported by the Directorate General of Higher Education, Research, and Technology, Ministry of Education, Culture, Research, and Technology of Indonesia for the fiscal year 2024 (Grant No. 027/E5/PG.02.00.PL/2024).

https://doi.org/10.17221/27/2025-JFS

Despite their importance, studies on tree root systems remain scarce and are often less thoroughly analysed than aboveground tree structures due to the challenges of *in-situ* observations and methodological constraints (Brunner et al. 2015). Roots are a form of woody biomass with inherent material density, which allows them to be detected based on sound wave velocity. Sound wave velocity refers to a mechanical longitudinal wave that requires a medium to propagate (Bucur 2006). Non-destructive techniques provide a viable solution, allowing root examination without damage, ensuring long-term safety and sustainability (Buza, Divós 2016).

Root detector is a technology designed to identify and map tree roots non-destructively. It operates based on sound wave velocity principles, specifically the time-of-flight difference between wave propagation through roots and soil (Rahman et al. 2021). Validation is a critical step in assessing the accuracy of the root detector. Previous studies by Rahman et al. (2021) and Taufiqurrachman et al. (2023) have verified a root detector using photogrammetry on exposed roots. However, the research of Rahman et al. (2021) remains an estimation method, as it is limited to visible surface roots. Excavation-based validation was conducted by Proto et al. (2020), revealing that a depth of 30 cm marks the detection limit, and a detection radius of 80 cm from the tree centre exhibits the highest correlation with root biomass. However, the accuracy value of the root detector has not been determined, limiting the validation of the root distribution. The primary objective of this research is to assess the accuracy of the radial distribution, including both buried and exposed roots, as obtained from the root detector tool using the excavation method.

MATERIAL AND METHODS

Sampling and site description. This research was conducted in the Gunung Walat Educational Forest (HPGW), Sukabumi Regency, West Java, Indonesia. Geographically, it is located at 6°54'23"S–6°55'35"S and 106°48'27"E–106°50'29"E (Nandi 2013). The tree used as a sample in this study was *Agathis loranthifolia* Salisb., which grows in flat terrain (0–5%) areas. Six trees growing close together were selected, consisting of three trees with buried roots (AG01, AG02, AG03) and three trees with exposed roots (AG04, AG05, AG06) (Figure 1). Morphometric parameters were live crown ratio (*LCR*) and mean crown diameter (*DCR*), measured as referred by Karlinasari et al. (2021). *LCR* is an indirect measure of a tree's ability to photosynthesise and a key indicator of its competitive position within the stand, while *DCR*, related to open spaces, enhances light availability, promoting greater crown expansion.

Analysis of site conditions. Soil physical properties were analysed to understand the growing conditions of the sampled trees. The sample to determine physical properties of the soil was taken out by the gravimetric method using a ring sample with a distance from the centre of the trunk of 80 cm and 150 cm at two depths (10–20 cm and 20–30 cm) and in two directions (north and south). The parameters used in the test of soil physical properties are bulk density (*BD*), porosity (*Po*), and soil moisture content (*SMC*), referring to Kurnia et al. (2022). The soil sample in the ring was weighed to determine the weight of fresh soil and ring (W_{fs}). The soil was baked for 24 hours at 105 °C and then weighed again to determine the weight of oven-dried soil (W_{ds}). The calculation of soil physical properties based on Kurnia et al. (2006) is shown in Equations (1–3):

$$BD = \frac{W_{ds}}{V_s} \quad (1)$$

$$Po = \left(1 - \frac{BD}{2.65}\right) \times 100\% \quad (2)$$

$$SMC = \frac{\left(W_{fs} - W_r\right) - W_{ds}}{W_{ds}} \times 100\% \quad (3)$$

where:

BD – bulk density (g·cm^{-3});
W_{ds} – weight of oven-dried soil (g);
V_s – volume of the soil sample (cm^3);
Po – porosity (%);
2.65 – soil particle density (g·cm^{-3});
SMC – soil moisture content (%);
W_{fs} – weight of fresh soil + ring (g);
W_r – weight of the ring (g).

Analysis of radial root distribution using a root detector. Detection of the root presence using a root detector was conducted at a position of 80 cm from the centre of the trunk outward. Meanwhile, a distance of 100 cm outward from the

https://doi.org/10.17221/27/2025-JFS

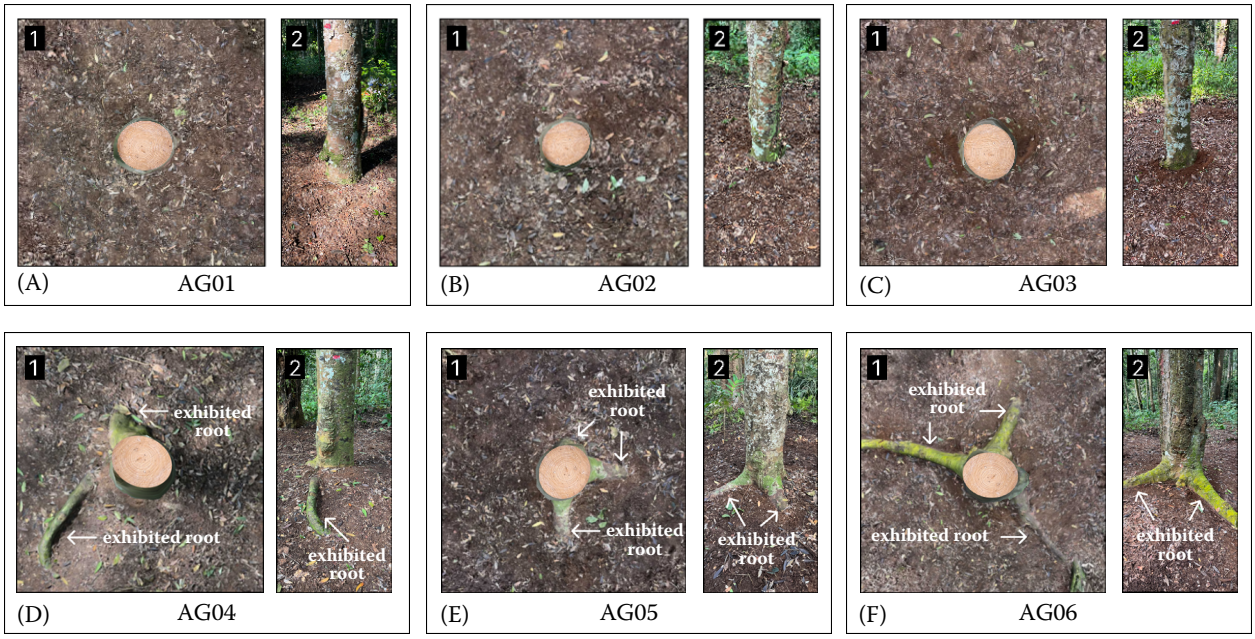

Figure 1. Tree samples of *Agathis* with (A–C) buried roots, and (D–F) exhibited roots

[1]visualisation of the lower part of the tree using KIRI engine; [2]lower part of the tree in the field

trunk was used as the boundary for the excavation area. Previous studies found that the optimal distance for detecting the radial distribution of tree roots is 80 cm from the tree trunk centre (Proto et al. 2020). A marker point at a distance of 150 cm was created as a guideline to ensure that the testing boundary aligns accurately with the testing rotation direction (Figure 2).

The Fakopp® root detector (Fakopp, Hungary) used in this study consists of two primary sensors: the receiver sensor (soil sensor) and the transmitter sensor (start sensor). The receiver sensor is embedded in the soil, while the transmitter sensor is positioned at the root collar. The receiver sensor is placed at a distance of 80 cm from the trunk centre, ensuring that the actual separation between the receiver sensor and the root collar is 80 cm minus the root collar radius (Figure 2A). Both sensors are arranged at an approximate angle of 45° – the receiver sensor relative to the soil surface and the transmitter sensor relative to the tree trunk. The sensor arrangement adheres to the specifications outlined in the Root Detector Manual 2.7 (Fakopp Enterprise 2019).

The root detection system operates by generating sound waves through a hammer strike on the transmitter sensor, with the receiver sensor capturing the propagated waves. This hammering process is performed three times to ensure consistent travel time propagation measurements. The assessment begins

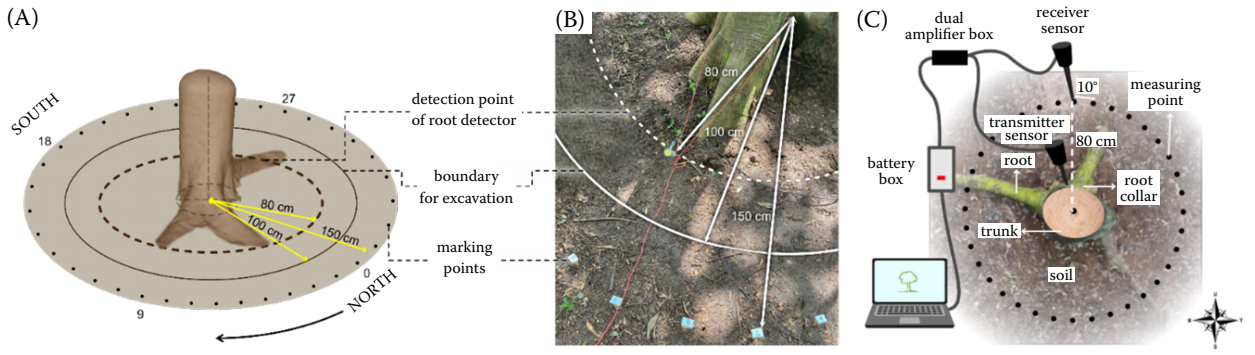

Figure 2. (A) Schematic illustration of the root detection and excavation boundaries, (B) field setup with marking points and measurement distances, and (C) root detector tool installation

https://doi.org/10.17221/27/2025-JFS

from the north side of the tree at a zero-degree point and continues clockwise around the trunk, with measurements taken every 10° (approximately 14 cm), leading to a total of 36 detection points (Proto et al. 2020) (Figure 2). The results are expressed in terms of sound velocity (V). The method of estimating the root presence based on sound velocity characteristics was based on Rahman et al. (2023) and Taufiqurrachman et al. (2023); it included values exceeding the 400 m·s^{-1} threshold, average velocities, and peak velocity measurements.

Accuracy analysis of root distribution based on the excavation method. The next stage after root detection through the root detector is to identify the actual root distribution through soil excavation around the roots. The excavation is conducted manually with traditional equipment of a hoe, shovel, and garden fork at a 100 cm radius from the centre of the trunk and at a depth of 30 cm. The soil excavation is carried out gradually across four tree areas to minimise the root damage (Sun et al. 2023). After excavating the tree roots to a depth of 30 cm below the surface, some root parameters were measured, including diameter, inclination angle, and depth. Measurements were conducted at a distance of 80 cm from the centre of the trunk (at the detection point) using a calliper and tape measure for diameter and depth, and a digital inclinometer (ATuMan, China) for the inclination angle. The roots that have been measured are classified according to Table 1.

In this study, root samples were collected from the lateral roots of trees for the analysis of physical properties, including root moisture content and root density. The samples of an approximate size of ± (2 × 2 × 1) cm were cut manually using a machete. Sampling was conducted in triplicate from different lateral roots. The selection of lateral roots was based on different cardinal directions or non-adjacent positions, following a modification of the method described by Taufiqurrachman et al. (2023). The fresh weight of the root samples (W_{fr}) was recorded, and their volume (V_r) was determined using Archimedes' principle. The root samples were then oven-dried at 105 °C for 24 hours until a constant weight was achieved, representing the dry weight (W_{dr}). The physical properties of the roots were calculated using Equations (4) and (5):

$$\rho = \frac{W_{fr}}{V_r} \tag{4}$$

$$RMC = \frac{W_{fr} - W_{dr}}{W_{dr}} \times 100\% \tag{5}$$

where:

ρ – root biomass density (g·cm^{-3});
W_{fr} – fresh weight of the root samples ;
V_r – volume of the root samples;
RMC – root moisture content (%);
W_{dr} – dry weight.

The accuracy was evaluated using a binary classification approach. The accuracy of the root distribution detection by a root detector was quantified using the overall accuracy (OA) percentage, calculated based on four evaluation metrics: true positive (TP), true negative (TN), false positive (FP), and false negative (FN), following the method described by Farhadpour et al. (2024), see Equation (6):

$$OA = \left(\frac{TP + TN}{TP + TN + FP + FN} \right) \times 100\% \tag{6}$$

where:

OA – overall accuracy (%);
TP – true positive (number of root objects correctly identified as roots);
TN – true negative (number of non-root objects correctly identified as non-roots);
FP – false positive (number of non-root objects incorrectly identified as roots);
FN – false negative (number of root objects incorrectly identified as non-roots).

Table 1. Classification of roots based on diameter, angle of inclination and depth

Parameter	Diameter	Inclination	Root depth
Classification	large (≥ 5 cm) medium (2–5 cm) small (< 2 cm)	horizontal (< 30°) oblique (30–50°) vertical (> 50°)	shallow (10–20 cm) deep (> 20 cm)
Source	–	Danjon et al. (1999)	modified from Danjon et al. (1999)

https://doi.org/10.17221/27/2025-JFS

Three-dimensional visualisation of root distribution. This study employed 3D Gaussian Splatting (3DGS) to reconstruct the three-dimensional (3D) distribution of tree roots. Gaussian splatting is a technology used in 3D image generation and modelling that enables the real-time rendering of 3D objects or scenes (Do et al. 2024). A 12 MP smartphone camera (f/1.6) (Apple Inc., USA) and the KIRI Engine application (Version 3.12.1, 2024) (KIRI Engine 2023) were used as the primary tools. The input data consisted of a 2-minute video capturing the tree root system. Video recording was conducted at a distance of 20–50 cm from the roots, following an orbital path around the base of the tree. The resulting 3D image was then overlaid with graphical data representing the root distribution based on acoustic wave velocity measurements obtained from the root detector.

Data analysis. Analysis of variance (ANOVA) and the Kruskal-Wallis test were employed to assess differences in the mean values of the parameters. Linear regression and Pearson correlation analyses were conducted to examine the relationships between sound velocity (*V*) and root parameters. The chi-square test was performed to evaluate the accuracy of the root detector in correctly identifying the number of detected roots.

RESULTS AND DISCUSSION

Tree morphometry and site conditions. The statistical analysis showed that tree height, *DCR*, *LCR*, root physical properties, soil bulk density, and soil porosity did not differ significantly at a 5% significance level between the sample trees. However, *DBH* and soil moisture content exhibited significant differences, with *P*-values < 0.05 (Table 2). Trees with buried roots exhibited lower *DBH* and total height compared to those with exposed roots (Table 2). According to Hammond (2023), root emergence on the soil surface is primarily due to the low soil oxygen availability. Research by Gilman et al. (1987) indicates that trees experiencing oxygen depletion tend to develop shallower root systems compared to those growing in well-oxygenated conditions. Under similar soil porosity conditions, trees with exposed roots have greater access to oxygen compared to those with buried roots, which may result in better growth performance. Based on morphometric parameters, trees with exposed roots had a larger mean crown diameter (*DCR*) of 6.17 m, compared to 5.83 m in trees with buried roots. This further supports the relation that trees with exposed roots exhibit better growth than those with buried roots. There was a correlation between the tree *DBH* and the *DCR*, as reported by Karlinasari et al. (2021) on the rain tree (*Samanea saman*).

Table 2. Summary of the growth and morphometric characteristics of *Agathis* trees

Tree	Root appearance	Morphometric parameters				Root physical properties		Soil physical properties		
		DBH (cm)	total height (m)	*DCR* (m)	*LCR*	ρ (g·cm^{-3})	*RMC* (%)	*BD* (g·cm^{-3})	*Po* (%)	*SMC* (%)
AG01	buried	35.03	18.00	4.75	0.56	0.81	114.66	0.78	70.51	54.71^{b}
AG02	buried	30.25	17.90	7.75	0.78	0.83	110.86	0.74	71.98	57.80^{ab}
AG03	buried	33.44	22.70	5.00	0.65	0.82	91.03	0.75	71.80	62.47^{ab}
AG04	exposed	40.76	31.80	8.00	0.87	0.80	113.34	0.72	72.80	64.42^{a}
AG05	exposed	38.22	22.00	5.25	0.59	0.84	103.53	0.71	73.19	65.87^{a}
AG06	exposed	47.13	20.00	5.25	0.40	0.92	84.11	0.78	70.66	64.61^{a}
Average	buried	32.91^{b}	19.53	5.83	0.66	0.82	105.51	0.76	71.43	58.33^{b}
	exposed	42.04^{a}	24.60	6.17	0.62	0.86	100.33	0.74	72.22	64.97^{a}
P-value	individual tree	0.42^{ns}	0.42^{ns}	0.42^{ns}	0.42^{ns}	0.96^{ns}	0.53^{ns}	0.62^{ns}	0.62^{ns}	0.01*
	root appearance	0.04*	0.27^{ns}	0.81^{ns}	0.79^{ns}	0.40^{ns}	0.67^{ns}	0.47^{ns}	0.44^{ns}	0.05*

*significant at the 5% level; ^{a,b}statistically significant differences; ^{ns}not significant; *DBH* – diameter at breast height; *DCR* – mean crown diameter; *LCR* – live crown ratio; ρ – root biomass density; *RMC* – root moisture content; *BD* – bulk density; *Po* – soil porosity; *SMC* – soil moisture content

https://doi.org/10.17221/27/2025-JFS

Meanwhile, the difference in average *LCR* values between the two groups was minimal (Table 2).

ANOVA revealed no significant differences in the root moisture content (*RMC*) and root biomass density (ρ) between the sampled trees (Table 2). This suggests that the root physical properties across the studied trees are relatively uniform, leading to a consistent effect on sound velocity propagation through the roots. Tree AG01 exhibited the lowest soil moisture content (Table 2) among all samples. Although AG01 was located on flat terrain, it was situated between sloping areas, allowing water to drain more easily. The surface water flow on sloping land tends to move faster due to gravity, resulting in the lower water infiltration capacity in the surrounding soil (Aryanto, Hardiman 2017; Banjarnahor et al. 2018). Conversely, soil moisture in exposed tree roots was higher than in buried roots (Table 2). According to Torreano and Morris (1998), roots generally tend to grow closer to the soil surface in moist soil conditions, whereas in dry soil, the root growth tends to shift deeper due to limited surface moisture. Meanwhile, *BD* and *SMC* did not show any significant differences.

Root distribution by root detector. The results of the study indicated that there were no statistically significant differences in overall sound wave velocity (*V*) between individual trees or in root visibility. However, a significant difference was observed in *V* suspected to propagate through roots (V_{root}) (Table 3). The mean and minimum values of V_{root} were higher in trees with exposed roots compared to buried roots (Table 3). The elevated V_{root} values in exposed tree roots are attributed to the generally higher overall sound wave velocity (*V*) in these trees, which consequently increases the threshold value used in root detection estimation (Rahman et al. 2023).

Radial distribution accuracy. The root detection results obtained from the root detector showed a lower number of detected roots compared to the actual root count based on soil excavation (Figure 3A). Trees AG02 and AG06 exhibited the greatest discrepancies in root count compared to other trees (Figure 3A). In tree AG02, all large-diameter roots (≥ 5 cm) were successfully detected; however, the number of the detected medium (2–5 cm) and small (< 2 cm) diameter roots was considerably lower (Table 4). According to Buza and Divós (2016), the detection threshold of the root detector is typically around 4 cm in diameter. Nevertheless, in this study, roots with diameters below 4 cm were detected, although the detection rate for small and medium roots remained lower than for large roots.

In contrast, tree AG06 had no small or medium roots present based on ground truth data, and the low detection rate was observed for large-diameter roots (Table 4). The limited detection frequency in this case is likely due to the root detection estimation method, which filters out non-peak velocity (*V*) values, thereby limiting the ability of the tool to detect closely spaced roots. In AG06, large roots were distributed in close proximity to one another (Figure 4F). Other sample trees also had closely spaced roots, but primarily of small to medium diameter, which were not detected using the acoustic wave velocity-based estimation (Figure 4A–E).

Table 3. The average, minimum, and maximum values of *V* and V_{root}

Tree	Root appearance	V (m·s^{-1})			V_{root} (m·s^{-1})		
		average	min.	max.	average	min.	max.
AG01	buried	477.58	198.00	1 517.00	802.29	485.00	1 517.00
AG02	buried	483.92	128.00	1 091.00	701.00	517.00	1 091.00
AG03	buried	437.11	127.00	1 361.00	949.80	470.00	1 391.00
AG04	exposed	535.17	160.00	1 054.00	913.88	607.00	1 054.00
AG05	exposed	499.31	118.00	1 450.00	1 166.33	698.00	1 450.00
AG06	exposed	595.22	137.00	1 303.00	915.56	616.00	1 303.00
Average	buried	466.20	151.00	1 323.00	817.70^{b}	490.67^{b}	1 323.00
	exposed	543.23	138.33	1 269.00	998.59^{a}	640.33^{a}	1 269.00
P-value	individual tree	0.38^{ns}	0.42^{ns}	0.42^{ns}	0.09^{ns}	0.42^{ns}	0.42^{ns}
	root appearance	0.07^{ns}	0.66^{ns}	0.77^{ns}	0.04*	0.01*	0.77^{ns}

*significant at the 5% level; ^{a,b}statistically significant differences; ^{ns}not significant; *V* – overall sound wave velocity in 36-point detection (m·s^{-1}); V_{root} – sound wave velocity suspected to propagate through roots (m·s^{-1})

https://doi.org/10.17221/27/2025-JFS

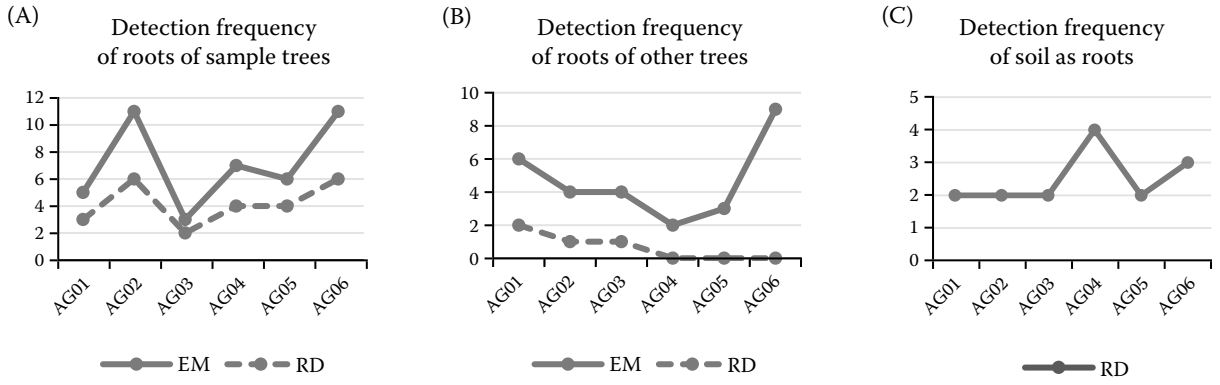

Figure 3. (A) Detection frequency of roots of the sample trees, (B) detection frequency of roots of other trees, and (C) detection frequency of soil as roots, based on excavation method (EM) and root detector (RD)

The roots detected by the root detector included not only those belonging to the sample trees themselves but also roots from neighbouring trees. However, the presence of roots from other trees was only detected in the group of trees with buried roots (Figure 3B). This phenomenon is likely due to the higher average *V* in trees with visible roots, resulting in a higher threshold for root detection based on mean *V* values. Roots from other trees, particularly those of small to medium diameter, tend to exhibit lower *V* values and thus they remained undetected. False positive detections, where the soil was mistakenly identified as root material, occurred across all sample trees. However, the rate of such misclassification was higher in trees AG04 and AG06 compared to the others (Figure 3C).

The regression analysis revealed that root diameter had the highest R^2 value compared to root depth and inclination. This indicates that 20.8% of the variation in root diameter can be explained by *V* (Table 5). The correlation test results demonstrated a positive relationship between all three variables and *V*. Among them, root diameter exhibited the highest correlation coefficient (0.456), followed by root inclination (0.320) and root depth (0.247) (Table 5).

Chi-square analysis revealed a significant relationship (*P*-value < 0.05) between the root detection results from the root detector and the excavation method, both in aggregate and when categorised by root appearance (Table 5). The accuracy of the root detector, regardless of the root visibility conditions, was 82.87%. When classified based on root visibility, the accuracy was slightly higher in trees with non-visible surface roots (83.33%) compared to those with visible roots (82.41%) (Table 6). However, both groups exhibited the accuracy values higher than 80%, with only a small difference between them. An accuracy rate of ≥ 80% for a non-destructive method like this is considered highly reliable and suitable for use under field conditions (Guo et al. 2013; Cristini et al. 2021).

Table 4. Root frequency of sample trees and other trees through the excavation method (EM) and detected by the root detector (RD), categorised by root diameter

Tree	Root frequency – sample trees						Root frequency – other trees					
	excavation method (EM)			root detector (RD)			excavation method (EM)			root detector (RD)		
	S	M	L	S	M	L	S	M	L	S	M	L
AG01	2	0	3	1	0	2	1	4	1	0	1	1
AG02	5	4	2	3	1	2	1	2	1	0	1	0
AG03	0	0	3	0	0	2	1	0	3	0	0	1
AG04	0	1	6	0	0	4	0	0	2	0	0	0
AG05	0	1	5	0	1	3	0	3	0	0	0	0
AG06	0	0	11	0	0	6	2	4	3	0	0	0

S – small-diameter roots (< 2 cm); M – medium-diameter roots (2–5 cm); L – large-diameter roots (≥ 5 cm)

https://doi.org/10.17221/27/2025-JFS

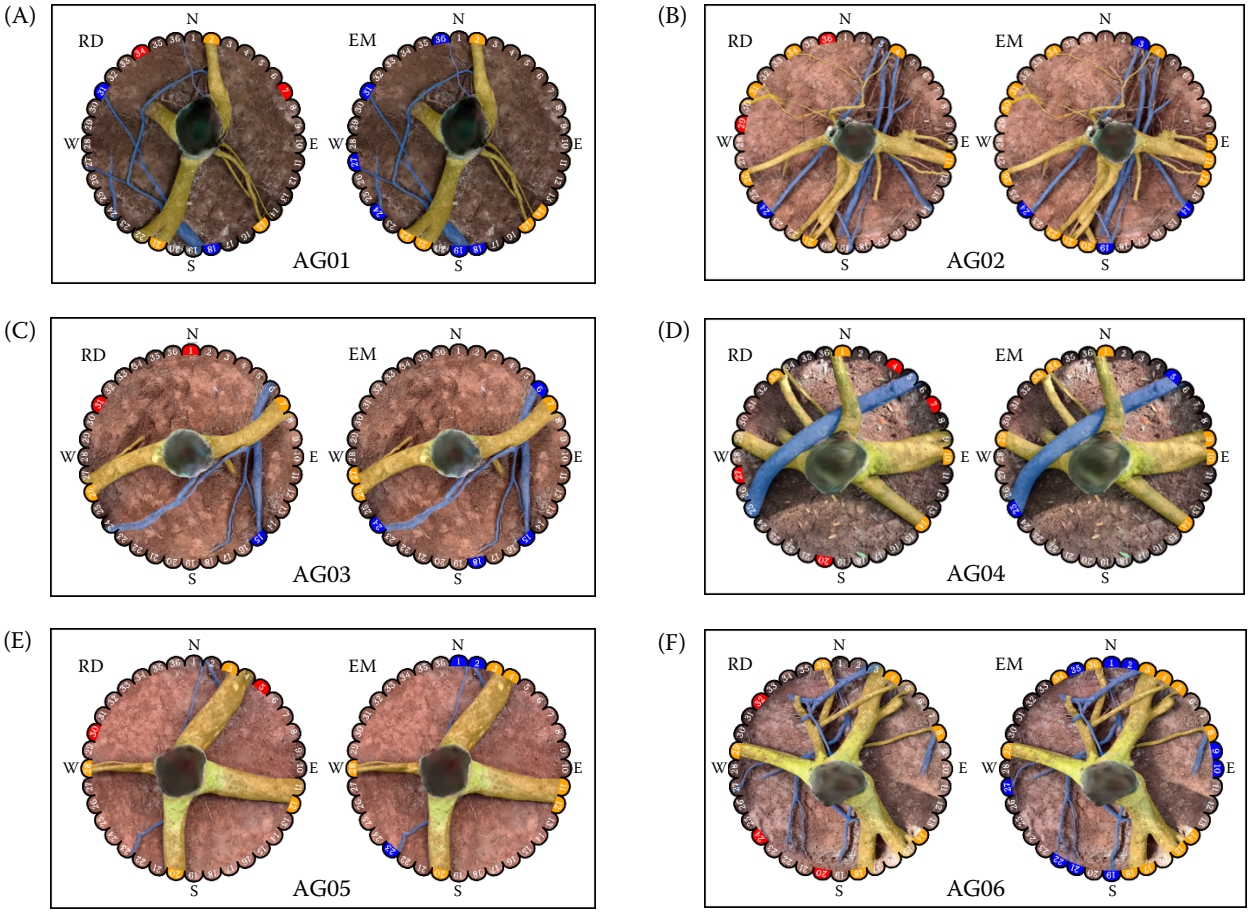

Figure 4. Overlaid image of root distribution by the root detector (RD) compared to excavation method (EM) on (A) AG01, (B) AG02, (C) AG03, (D) AG04, (E) AG05, and (F) AG06

Coloured points in the RD image represent root detector outputs identified as potential roots; colour differences indicate the type of object detected (yellow – sample tree roots; blue – other tree roots; red – soil); the EM image shows root identification results from the excavation method (yellow – sample tree roots; blue – other tree roots)

The accuracy of root detection as roots (true positive) was higher in trees with exposed roots (61%) compared to those with buried roots (52%) (Figure 5A, B). In contrast, the accuracy of non-root detection as non-roots (true negative) was higher in trees with buried roots (91%) than in those with exposed roots (88%). These findings indicate that root detection is more accurate in trees with exposed root systems compared to trees with covered or buried roots. The presence of the soil covering

Table 5. Regression analysis results of the sound wave velocity V, diameter, depth, and root inclination

No.	Regression model	Dependent variable (y)	Independent variable (x)	Intercept (β_0)	Coefficient (β_1)	R^2	Multiple R (Pearson's correlation)	Significance (P-value)
1	$y = 0.6153x - 39.229$	root diameter	sound wave velocity (V)	–39.229	0.615	0.208	0.456	0.000
2	$y = 0.0237x - 0.1191$	root depth	sound wave velocity (V)	–0.119	0.024	0.061	0.247	0.008
3	$y = 0.0431x - 3.1692$	root inclination	sound wave velocity (V)	–3.169	0.043	0.103	0.320	0.001

https://doi.org/10.17221/27/2025-JFS

Table 6. The chi-square test value of the root detector

Chi-square test	Number of points	Chi-square (Pearson)	*df*	Accuracy rate	*P*-value
All trees (n = 6)	216	47.215	1	82.87%	0.000*
Trees with buried roots (n = 3)	108	21.762	1	83.33%	0.000*
Trees with exposed roots (n = 3)	108	25.254	1	82.41%	0.000*

*significance at the 5% level ($P < 0.05$); *df* – degree of freedom; n – number of trees

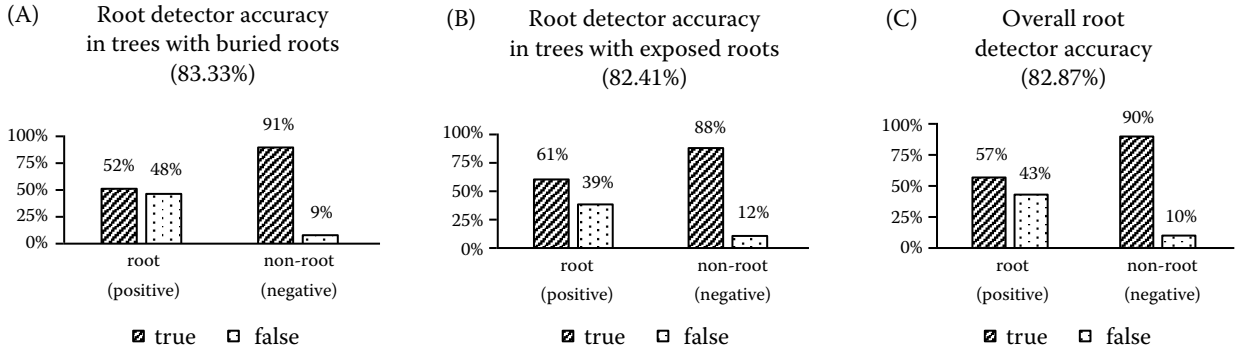

Figure 5. Graphs of the root detector accuracy values for (A) trees with buried roots, (B) trees with exhibited roots, and (C) overall root detector accuracy

the roots may reduce the accuracy of root detection, while improving the accuracy of soil detection as non-root. When viewed as a whole, regardless of the root appearance, the overall accuracy of detecting roots as roots was 57%, while detecting soil as soil reached 90% (Figure 5C). This shows that the accuracy of soil classification as non-root is substantially higher than that of root classification.

CONCLUSION

The Fakopp® root detector demonstrated reliable performance in estimating the tree root distribution, with an overall accuracy of 82.87%. The accuracy of detecting roots as roots in trees with exposed roots was higher (61.00%) compared to buried roots (52.00%). Conversely, the accuracy of detecting non-roots as non-roots was higher in exposed tree roots (91.00%) than in buried roots (88.00%). The study found that root diameter had the strongest correlation with sound velocity (R^2 = 20.8%). The root detector was capable of detecting roots belonging to the sample tree itself, including those with small (< 2 cm), medium (2–5 cm), and large (≥ 5 cm) diameters. However, in trees with buried root systems, roots from other trees were also detected by the device, particularly those of medium and large diameters.

Acknowledgement: The authors would like to express their sincere gratitude to the Competitive Grant Program from the Ministry of Education, Culture, Research, and Technology of Indonesia, for funding this research under the Master Research Scheme (PTM). We also extend our appreciation to the Gunung Walat Educational Forest, Faculty of Forestry and Environment, IPB University, for the research facilities.

REFERENCES

Abuseif M., Gou Z. (2018): A review of roofing methods: Construction features, heat reduction, payback period and climatic responsiveness. Energies, 11: 1–22.

Abuseif M., Dupre K., Michael R.N. (2021): The effect of green roof configurations including trees in a subtropical climate: A co-simulation parametric study. Journal of Cleaner Production, 317: 128458.

Aryanto D.E., Hardiman G. (2017): A multivariate study of factors affecting groundwater infiltration as a basis for determining potential groundwater recharge zones. Proceeding Biology Education Conference, 14: 252–257.

Banjarnahor N., Hindarto K.S., Fahrurrozi F. (2018): The relationship between slope and soil moisture content, soil pH, and performance of *Jeruk Gerga* in Lebong Regency. Jurnal Ilmu-Ilmu Pertanian Indonesia, 20: 13–18.

https://doi.org/10.17221/27/2025-JFS

Brunner I., Herzog C., Dawes M.A., Arend M., Sperisen C. (2015): How tree roots respond to drought. Frontiers in Plant Science, 6: 1–16.

Bucur V. (2006): Acoustics of Wood. Berlin, Springer: 394.

Buza Á.K., Divós F. (2016) Root stability evaluation with non-destructive techniques. Acta Silvatica et Lignaria Hungarica, 12: 125–134.

Cristini V., Tippner J., Vojáčková B., Paulić V. (2021): Comparison of variability in results of acoustic tomographs in pedunculate oak (*Quercus robur* L.). BioResources, 16: 3046–3058.

Currie B.A., Bass B. (2008): Estimates of air pollution mitigation with green plants and green roofs using the UFORE model. Urban Ecosystem, 11: 409–422.

Danjon F., Bert D., Godin C., Trichet P. (1999): Structural root architecture of 5-year-old *Pinus pinaster* measured by 3D digitising and analysed with AMAPmod. Plant Soil, 217: 49–63.

Do T.L.P., Choi J., Le V.Q., Gentet P., Hwang L., Lee S. (2024): HoloGaussian digital twin: Reconstructing 3D scenes with Gaussian splatting for tabletop hologram visualization of real environments. Remote Sensing, 16: 4591.

Fakopp Enterprise (2019): Manual for Root Detector. Ágfalva, Fakopp Enterprise: 1–16.

Farhadpour S., Warner T.A., Maxwell A.E. (2024): Selecting and interpreting multiclass loss and accuracy assessment metrics for classifications with class imbalance: Guidance and best practices. Remote Sensing, 16: 1–22.

Gilman E.F., Leone L.A., Flower F.B. (1987): Effect of soil compaction and oxygen content on vertical and horizontal root distribution. Journal of Environmental Horticulture, 5: 33–36.

Hammond E. (2023): Understanding Tree Roots: Functions of Tree Roots. CMG GardenNotes. Fort Collins, Colorado State University Extension: 6.

KIRI Engine (2023): Exploring Three Innovative 3D Scanning Methods: Manual Capturing, Auto Capturing, and Video Recording. Hong Kong, KIRI Innovations. Available at: https://www.kiriengine.app/blog/explained/exploring-three-innovative-3d-scanning-methods

Kurnia U., Agus F., Adimihardja A., Dariah A. (2006): Technical Manual for Soil Physical Analysis. Bogor, Indonesian Center for Agricultural Land Resources Research and Development: 261.

Kurnia U., Agus F., Adimihardja A., Rachman A., Sutono S., Santri J.A., Ariani R. (2022): Soil Physical Properties and Their Analytical Methods. 2nd Ed. Bogor, Indonesian Soil Research Institute: 303.

Mughal H., Corrao R. (2018): Role of sky-gardens in improving energy performance of tall buildings. In: International Conference on Seismic and Energy Renovation for Sustainable Cities (SER4SC), Catania, Feb 1–3, 2018: 1–9.

Nandi K. (2013): Gunung Walat Educational Forest, Management History (unpublished manuscript).

Proto A.R., Di Iorio A., Abenavoli L.M., Sorgonà A. (2020): A sonic root detector for revealing tree coarse root distribution. Scientific Reports, 10: 1–12.

Rahman M.M., Adzkia U., Rachmadiyanto A.N., Dwiyanti F.G., Nandika D., Nugroho N., Siregar I.Z., Karlinasari L. (2021): Coarse root distribution of *Vatica pauciflora* (Korth.) Blume in different soil slopes as revealed by root detector. IOP Conference Series: Earth and Environmental Science, 918: 012046.

Rahman M.M., Fredisa Y., Nandika D., Nugroho N., Siregar I.Z., Karlinasari L. (2023): Inferring vertical tree growth direction of *Samanea saman* and *Delonix regia* trees with the pattern of lateral root distribution using the root detector. Forests, 14: 1–14.

Smiley E.T. (2008): Root pruning and stability of young willow oak. Arboriculture and Urban Forestry, 34: 123–128.

Sun D., Jiang F., Wu H., Liu S., Luo P., Zhao Z. (2023): Root location and root diameter estimation of trees based on deep learning and ground-penetrating radar. Agronomy, 13: 1–18.

Taufiqurrachman M., Syafitri U.D., Rahman M.M., Siregar I.Z., Karlinasari L. (2023): Clarifying the main root distribution of trees in varied slope environments using non-destructive root detection. Forests, 14: 1–26.

Torreano S.J., Morris L.A. (1998): Loblolly pine root growth and distribution under water stress. Soil Science Society of America Journal, 62: 818–827.

Received: March 15, 2025
Accepted: August 7, 2025
Published online: August 27, 2025